Sedimentary Geology 341 (2016) 58–69

Contents lists available at ScienceDirect

Sedimentary Geology

journal homepage: www.elsevier.com/locate/sedgeo

Cambrian Series 3 carbonate platform of Korea dominated by microbial-sponge reefs

Jongsun Hong [a,1], Jeong-Hyun Lee [b,2], Suk-Joo Choh [a,*], Dong-Jin Lee [c,3]

[a] Department of Earth and Environmental Sciences, Korea University, Seoul 02841, Republic of Korea
[b] Department of Geology and Earth Environmental Sciences, Chungnam National University, Daejeon 34134, Republic of Korea
[c] Department of Earth and Environmental Sciences, Andong National University, Andong 36729, Republic of Korea

ARTICLE INFO

Article history:
Received 5 February 2016
Received in revised form 19 April 2016
Accepted 20 April 2016
Available online 2 May 2016

Editor: Dr. B. Jones

Keywords:
Microbial-sponge reef
Cambrian Series 3
Carbonate platform
Korea

ABSTRACT

Metazoans have been considered as negligible components of Cambrian Series 3 and Furongian microbial-dominated reefs, in contrast to their presence in earlier Terreneuvian–Cambrian Series 2 microbial–archaeocyath reefs. However, recent discoveries of sponges in Cambrian Series 3–Furongian reefs of Australia, China, Iran, USA, and Korea have raised question regarding their contribution in terms of carbonate platform development, which have never been assessed. This study examines Cambrian Series 3 deposits of the Daegi Formation, Korea to elucidate this question. The 100-m-thick middle part of the Daegi Formation is dominated by boundstone facies, which occupies 45% of the study interval, as well as bioclastic wackestone to packstone, bioclastic grainstone, and ooid packstone to grainstone facies. The Daegi reefs are primarily thrombolitic in composition, with 90% ($n = 26/29$) of the reefs containing an average of 9% sponges in aerial percentage calculated from thin sections. Lithistid sponges composed of peloidal fabrics, some desma spicules, and spicule networks commonly occupy the interstitial space in microbial clusters, are encrusted by mesoclots and *Epiphyton*, and are surrounded by micrite. Subordinate non-lithistid demosponges occur within clusters of microbial elements. The middle Daegi Formation can be largely subdivided into shoal environment dominated by grainstone to packstone facies and shallow subtidal platform interior environment located behind shoal with wackestone to packstone facies. The microbial-sponge reefs mainly developed around platform interior as patch reefs. The current study indicates that metazoans in the form of lithistid and non-lithistid demosponges are nearly ubiquitously incorporated in Daegi reefs and contributed greatly to the formation of microbial-sponge reefs as well as carbonate platform during the time. Study of these microbial-sponge reefs and their distribution within the carbonate platform may help us to understand how carbonate sedimentary environments responded to the extinction of archaeocyaths.

1. Introduction

The early Palaeozoic marked a grand shift in the evolution of reefs, from primarily microbial reefs to metazoan-dominated skeletal reefs (Wood, 1999; Rowland and Shapiro, 2002; James and Wood, 2010). The first Phanerozoic reefs with widespread metazoan component (mainly archaeocyath) emerged on the Siberian Platform in the late Terreneuvian; these reefs flourished for up to 15 m.y., until their extinction in the late early Cambrian (Cambrian Series 2; middle Stage 4) (Riding and Zhuravlev, 1995; Rowland and Shapiro, 2002; Gandin and Debrenne, 2010). The combined impacts of late Cambrian Series 2 anoxia and global regression sharply reduced the microbial-archaeocyath reefs (Zhuravlev, 1996; Flűgel and Kiessling, 2002; Rowland and Shapiro, 2002), resulting in the subsequent dominance of thrombolite and dendrolite microbial reefs with *Epiphyton*, *Renalcis*, and *Girvanella* (Lee et al., 2015). However, reports during the last decade from China, Australia, Iran, USA, and Korea have revealed the presence of anthaspidellid sponges and other metazoans including non-lithistid demosponges, heteractinide sponges, and stem-group cnidarians in middle–late Cambrian (Cambrian Series 3–Furongian) reefs in these regions, resulting in the speculation that metazoans may have been much more common and widely distributed in middle–late Cambrian "microbial-dominated" reefs than previously thought (Shapiro and Rigby, 2004; Johns et al., 2007; Kruse and Zhuravlev, 2008; Hong et al., 2012; Kruse and Reitner, 2014; Lee et al., 2014, in press; Adachi et al., 2015). It is therefore necessary to re-assess these reefs as well as surrounding depositional environments in order to understand how such conditions affected formation of carbonate platforms during the time. In this study, we assess and document the presence and extent of metazoan constituents in microbial reefs of the Cambrian Series 3 Daegi Formation, Korea, and their depositional environments. The

* Corresponding author. Tel.: +82 2 3290 3180; fax: +82 54 822 5467.
E-mail addresses: bulgeun@korea.ac.kr (J. Hong), jeonghyunlee@cnu.ac.kr (J.-H. Lee), sjchoh@korea.ac.kr (S.-J. Choh), djlee@andong.ac.kr (D.-J. Lee).
[1] Fax: +82 2 3290 3189.
[2] Fax: +82 42,822 7661.
[3] Fax: +82 54,822 5467.

http://dx.doi.org/10.1016/j.sedgeo.2016.04.012
0037-0738/

presence of sponges throughout the Cambrian Series 3 reefs could significantly change our perception of the evolutionary patterns of early Palaeozoic reefs as well as carbonate platforms.

2. Geological setting and methods

Extensive early Palaeozoic epeiric carbonate platforms developed on the Sino–Korean Block, located on the eastern margin of Gondwana near present-day Australia and India (McKenzie et al., 2011). A Cambro–Ordovician succession on the block occurs in the area of northern to northeastern China and Korea, spanning an area up to 2000 km east–west and 1000 km north–south (Meng et al., 1997) (Fig. 1A). The Taebaek Group, located on the eastern margin of the platform, consists of ten formations, distinguished by the dominance of sandstone, shale, limestone, and limestone–shale interbeds (Chough, 2013). The Daegi Formation (150–250 m thick), the lowest carbonate-dominant unit of the Taebaek Group, is composed of shale and nodular limestones in lower part and ooid and bioclastic limestones in the middle to upper part, and is interpreted as off-platform to shallow subtidal platform deposits, respectively (Choi et al., 2004; Kwon et al., 2006; Sim and Lee, 2006; Hong et al., in press). The identification of *Crepicephalina*, *Amphoton*, and *Jiulongshania* trilobite biozones in the formation indicates a late Stage 5–middle Guzhangian age (Geyer and Shergold, 2000; Kang and Choi, 2007; Park et al., 2008; Peng et al., 2012) (Fig. 1B).

The study area is located 17 km southeast of Taebaek, where the 180-m-thick Daegi Formation outcrops (Fig. 1A). In this study, we focus on the middle part of the Daegi Formation (40–140 m interval). This interval was measured and sampled at an average vertical spacing of 21 cm; additional samples were collected from reef intervals. More than 700 standard (2.7 cm × 4.9 cm) and large (5.2 cm × 7.6 cm) format thin sections prepared from more than 600 samples were used to identify and log fabrics, constituent types, and their proportions by visual

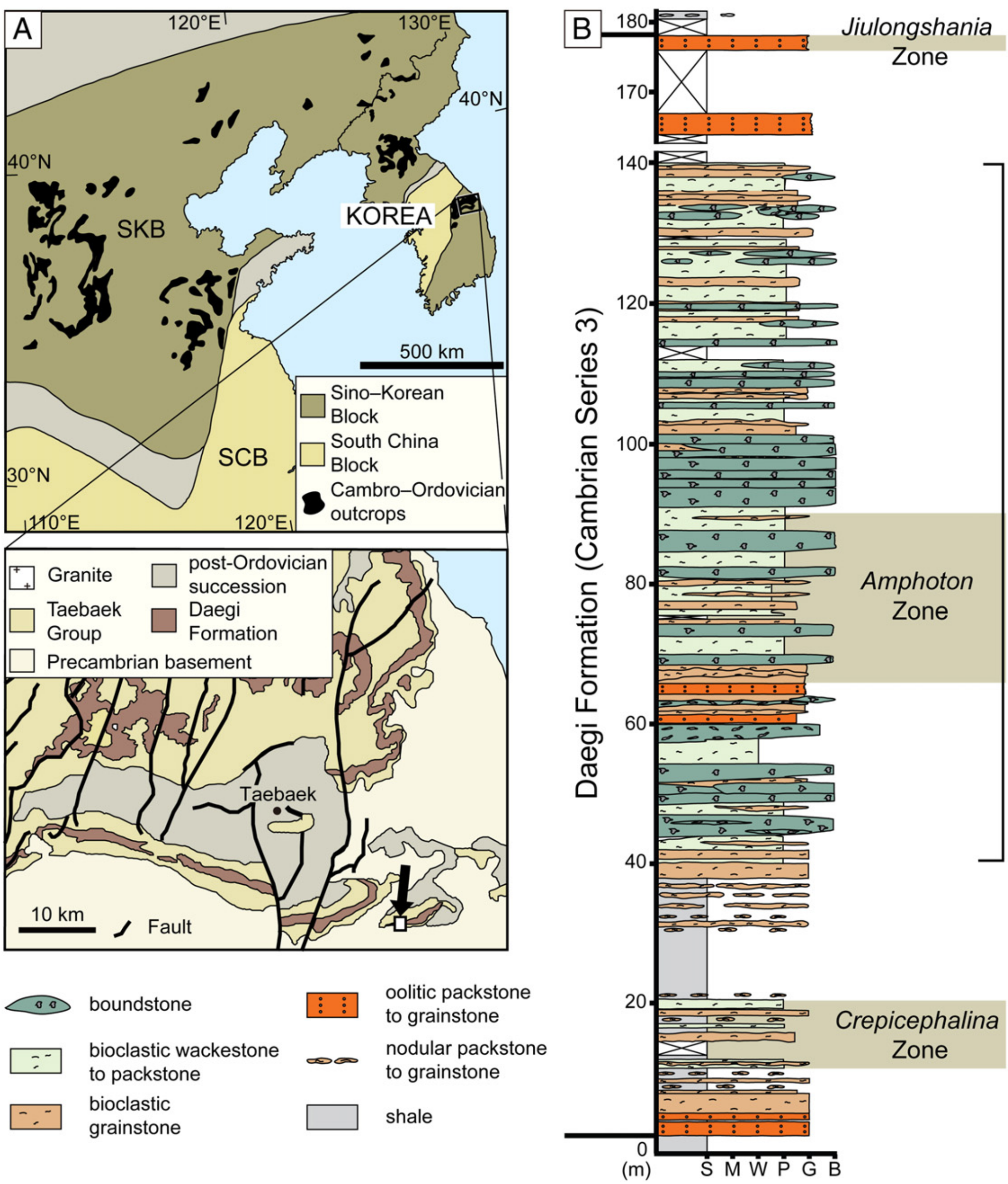

Fig. 1. (A) Tectonic elements of East Asia, showing the distribution of Cambro–Ordovician outcrops in the Sino–Korean Block and geologic map of the Taebaek Group in eastern Korea. The study area is marked by a black arrow. Modified from Sim and Lee (2006) and Chough (2013). (B) Measured section of the Daegi Formation in the study area. Modified after Hong et al. (in press).

estimation (Flűgel, 2010) (Fig. 2). Texture of microbial-sponge reefs is mapped on the thin sections and aerial percentage of constituents are calculated based on these maps. The white card technique (Delgado, 1977; Folk, 1987) was routinely employed to enhance recognition of organic matter-rich siliceous sponge spicule networks.

3. Results

The middle Daegi Formation is dominated by carbonate facies including bioclastic wackestone to packstone, ooid packstone to grainstone, and bioclastic grainstone, as well as several boundstone facies (Table 1) (Hong et al., in press). Due to poor outcrop condition, sedimentary facies are identified based on microscale observation. Thirty-two microbial reefs are identified from the middle Daegi Formation (Fig. 2). Collectively, the cumulative thickness of the reefs is 45% of the thickness of the study interval. The majority of the reefs ($n = 29/32$) are composed of thrombolite-sponge boundstone. These thrombolitic patch reefs are recognized in the field by their massive appearance and clotted fabric (Sim and Lee, 2006; Hong et al., 2012). Less than half ($n = 12/29$) of the thrombolitic reefs are decimetre-scale bodies, and more than four fifths ($n = 24/29$) are <2 m thick. The reefs are intercalated with bioclastic wackestone to packstone and bioclastic

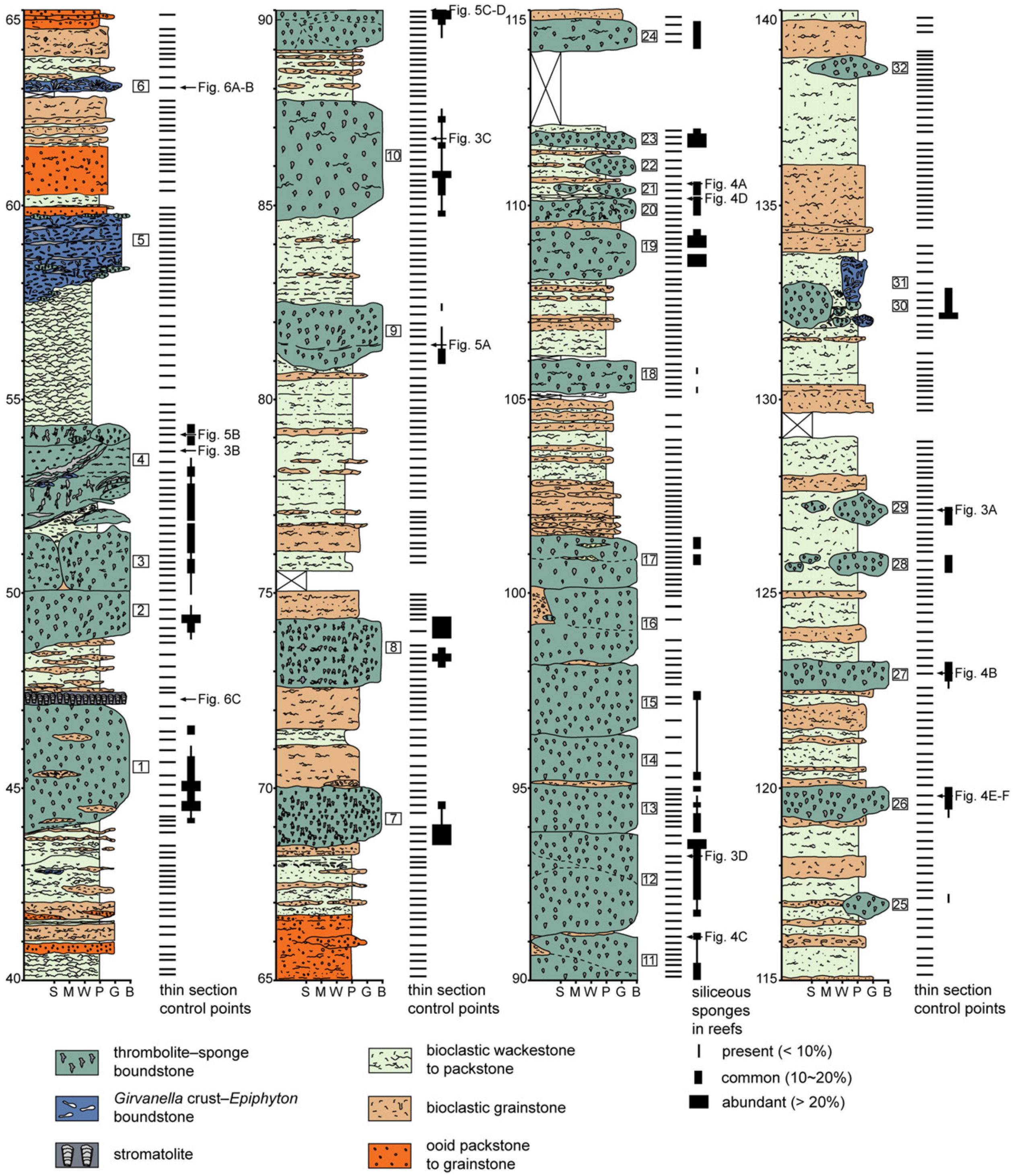

Fig. 2. Columnar section of the 40- to 140-m interval of the Daegi Formation. Sample points and relative proportion of sponges in reefs are marked on the right of column.

Table 1
Summary of sedimentary facies of the middle Daegi Formation (modified after Hong et al., in press).

Facies	Description	Interpretation
Boundstone	Thrombolite-sponge boundstone several cm to 3.3 m in thickness, *Girvanella* crust-*Epiphyton* boundstone several cm to 2.2 m in thickness, Stromatolite 0.2 m in thickness; Associated with bioclastic wackestone to packstone and grainstone and ooid packstone to grainstone	Shallow subtidal platform, behind grainstone shoal to platform interior
Bioclastic wackestone to packstone	Medium to very thick beds (0.1–3.7 m) with common dissolution seams; Intercalation with boundstone and thin bedded bioclastic grainstone and ooid packstone to grainstone	Low energy shallow subtidal back shoal to platform interior
Bioclastic grainstone	Lenses and medium to very thick beds (0.1–2.2 m) with common erosive surfaces; Associated with bioclastic wackestone to packstone and boundstone; Common to abundant trilobites, eocrinoids and peloids; Rare chancelloriid sclerites, *Epiphyton*, sponge spicules, sponge spicule networks, and *Girvanella* crusts	Platform margin shoal
Ooid packstone to grainstone	Amalgamated medium to very thick beds and lenses (0.1–2 m); Associated with bioclastic wackestone to packstone and boundstone; Abundant ooids and subordinate oncoids; Rare trilobites, eocrinoids, brachiopods, chancelloriid sclerites, intraclasts, calcimicrobes and sponges spicules	Platform margin shoal

grainstone facies (Table 1; Fig. 2). The intercalated facies contain trilobite fragments, peloids and less commonly eocrinoid ossicles. Sponge spicules, *Epiphyton*, *Girvanella* crusts, and chancelloriid sclerite fragments are rare.

3.1. Thrombolite-sponge boundstone

The thrombolite-sponge boundstone is composed mainly of dark to light grey micritic mesoclots (Fig. 3A and B), *Epiphyton*, and siliceous sponges. *Girvanella* crusts, the stem-group cnidarian *Cambroctoconus* (Hong et al., 2012; Park et al., in press) and *Renalcis*-like calcimicrobes, are minor constituents. Lime mud, rare trilobite fragments, eocrinoid ossicles, and scattered monaxon spicules occur in between these constituents within the boundstone. Globular to irregular or upward-widening, dark coalesced mesoclots 3–7 mm across (Fig. 3C) are composed of micrite with peloids 30–50 μm in diameter (e.g., Riding, 2000). *Epiphyton* with characteristic branching bushy micrites 20–55 μm in diameter often occurs in mesoclots, where bush-like bundles of *Epiphyton* gradationally co-occur with peloidal micrite. Some mesoclots would have been originated from *Epiphyton* thalli, based on similarities in their shapes and the presence of silicified *Epiphyton* at the outer margin of some clots (Fig. 3C). *Epiphyton* constitutes the bulk of the light-grey clots,

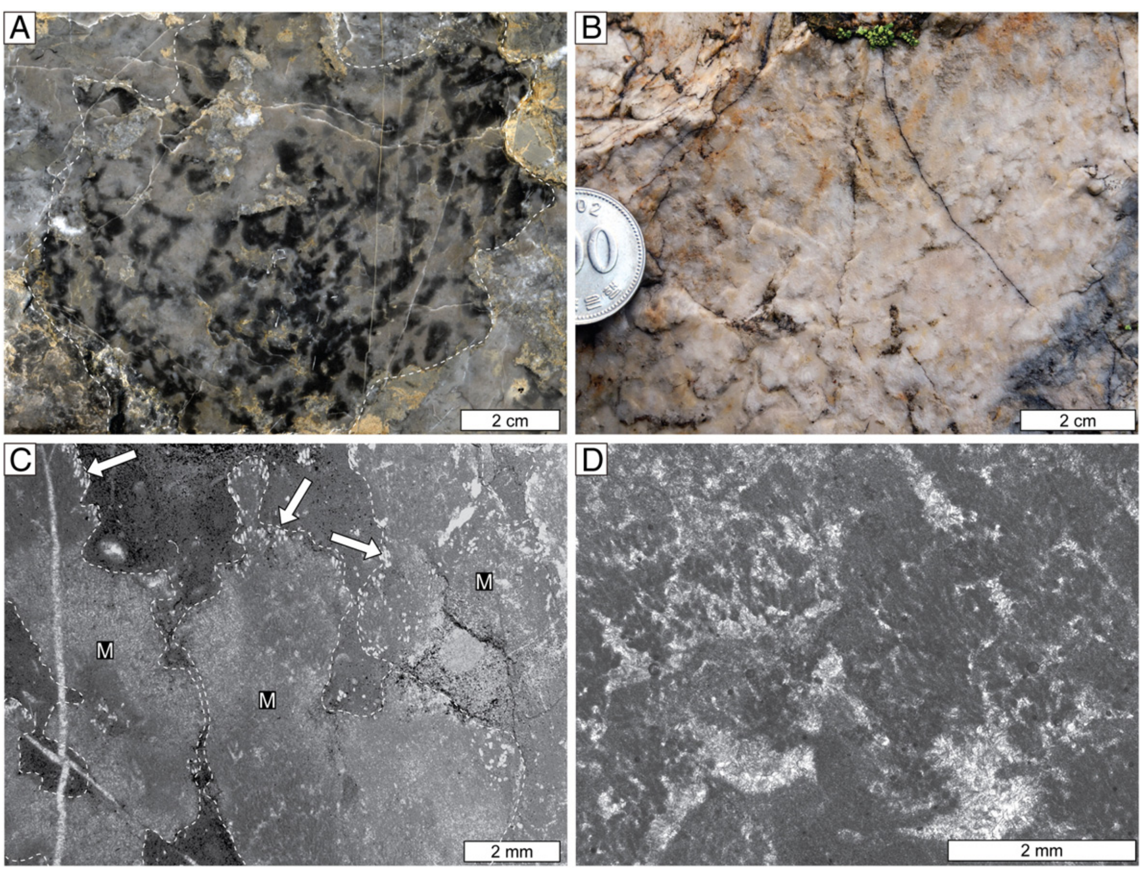

Fig. 3. Microbial elements of the thrombolite-sponge boundstone. (A) Slab photograph, showing dark micritic mesoclots surrounded by lighter coloured lime mud. (B) Outcrop photograph of pervasive white clots. (C) Photomicrograph of mesoclots. Some silicified *Epiphyton* filaments occur at the outer margin of some mesoclots (white arrows). (D) Photomicrograph of *Epiphyton* clusters growing upward on top of other thalli, partly overlain by internal sediments and surrounded by spar cement. M = mesoclots. Refer to Fig. 2 for sample locations.

which are surrounded by micritic sediment and microspar (Fig. 3D). Mesoclots and *Epiphyton* thalli produce loosely to densely clustered fabrics separated by a few millimetres to several centimetres (Figs. 3C and 5A–D). Vertically and laterally merging mesoclots, as well as their further amalgamation, results in larger bulbous to irregular microbial frameworks of up to several centimetres across. Some upward stacking of clots within columnar to branching frameworks results in forms similar to those of dendrolites (e.g., Howell et al., 2011).

Most thrombolitic reefs in the formation (90%; $n = 26/29$) contain siliceous sponges, which comprise, on average, 9% of the thrombolite-sponge boundstone and locally over 20% (Fig. 2). These sponges occur mostly as irregular patches of lime mudstone to peloidal packstone, making detailed taxonomic determinations difficult. Unidentified lithistid and non-lithistid demosponges are present in the boundstone, as determined by spicule shapes. This is the first documentation of lithistid sponges in the Daegi reefs and complements previously published reports of non-lithistid demosponges in the reefs (Hong et al., 2012).

Lithistid sponges, with desma spicules 20–110 μm in diameter and with enlarged spicule rays at their contacts (Fig. 4A–C), are up to 1.3 cm wide and occur as irregular patches with indistinct outlines (Fig. 4D and E). They are composed of spherical to angular peloidal clots 20–500 μm in diameter, either scattered or aligned in rows (Fig. 4D–F). These peloidal fabric gradationally changes into spicule

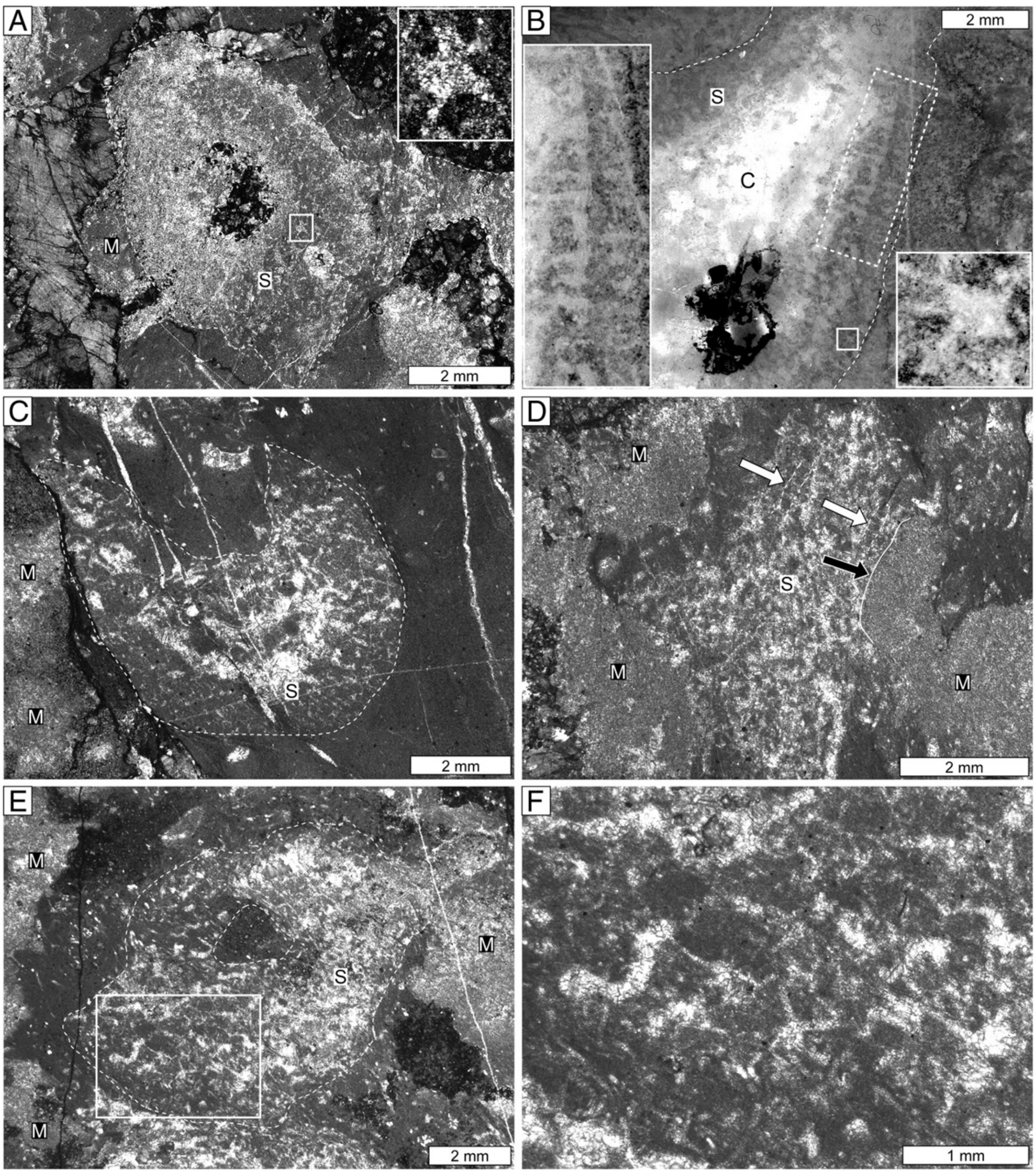

Fig. 4. Photomicrographs of the lithistid sponges in thrombolite-sponge boundstone. (A) Transverse section of rare conical sponge partly preserved as a network of spicules and peloidal fabric. Probable desma spicule with enlarged intersecting points of spicule rays is marked by a white rectangle and its enlargement in the upper right. (B) Desma spicules (white rectangle, shown in the enlarged insert in the lower right) and their ladder-like arrangements (dashed white rectangle; enlarged in the left), visualized using the white card technique (Delgado, 1977; Folk, 1987). (C) Conical sponge with some regular spicule arrays. (D) Partial sponge remains composed of peloids and randomly oriented spicules. The peloids are either scattered or aligned in a row (white arrows). The sponge remains laterally border mesoclots (black arrow), which follow the outline of the sponge. (E, F) Poorly preserved sponge remains composed of peloids and spicules. Enlargement of white rectangle shows angular to spherical peloids intermixed with ghosts of spicules. M = mesoclots; S = sponges; C = cement. Refer to Fig. 2 for sample locations.

networks with partially connected spicules with micrite (Fig. 4C) or is intermixed with randomly oriented and dissociated spicules (Fig. 4E and F). In rare cases, lithistid sponges occur as cylindrical to conical forms 0.4 to 1.4 cm in diameter and more than 2.7 cm long, with a smooth outer surface (Fig. 4A–C). Ladder-like arrays of spicules suggest their anthaspidellid affinity (Fig. 4B) (Lee et al., in press). The majority of lithistid remains occur between mesoclots and *Epiphyton* thalli and are surrounded by micrite (Figs. 4E and 5A). Rarely, lithistid sponges are attached to microbial clusters (Figs. 4D and 5B–D). Where lithistids laterally contact mesoclots and *Epiphyton* frameworks, the microbial elements conform to the outer surface of the sponges (Figs. 4D and 5B).

Non-lithistid demosponges with reticulate arrays of weakly curved spicules, with uniform diameters (60–70 μm) and lacking spicules connected at right angles to one another (fig. 5C in Hong et al., 2012). These non-lithistid demosponge remains are subordinate to lithistids and also occur as irregular patches with indistinct outlines, and with maximum dimensions of 0.4–1.7 cm. Their textures are similar to probable "keratose" demosponges (Luo and Reitner, 2014), but their exact taxonomic classification is still pending. These sponges are enclosed by dense clusters of *Epiphyton* thalli and are occasionally covered by lime mud (Hong et al., 2012).

3.2. Other microbial boundstones

In the Daegi Formation, three reefs composed of *Girvanella* crust–*Epiphyton* boundstone are intercalated with bioclastic wackestone to packstone, bioclastic grainstone, and ooid packstone to grainstone facies (Fig. 2). Several small lensoidal mounds of this boundstone are also present within the thrombolite-sponge reefs (Hong et al., 2012). Closely spaced sub-vertical to horizontally aligned sheet-like to arcuate *Girvanella* crusts 5–20 mm long and 0.1–1 mm thick are dominant components of the boundstone (Fig. 6A). Fan-shaped and some chambered *Epiphyton* thalli form microbial clusters up to 10 mm wide and several millimetres high, which encrust the upper surfaces of the *Girvanella*

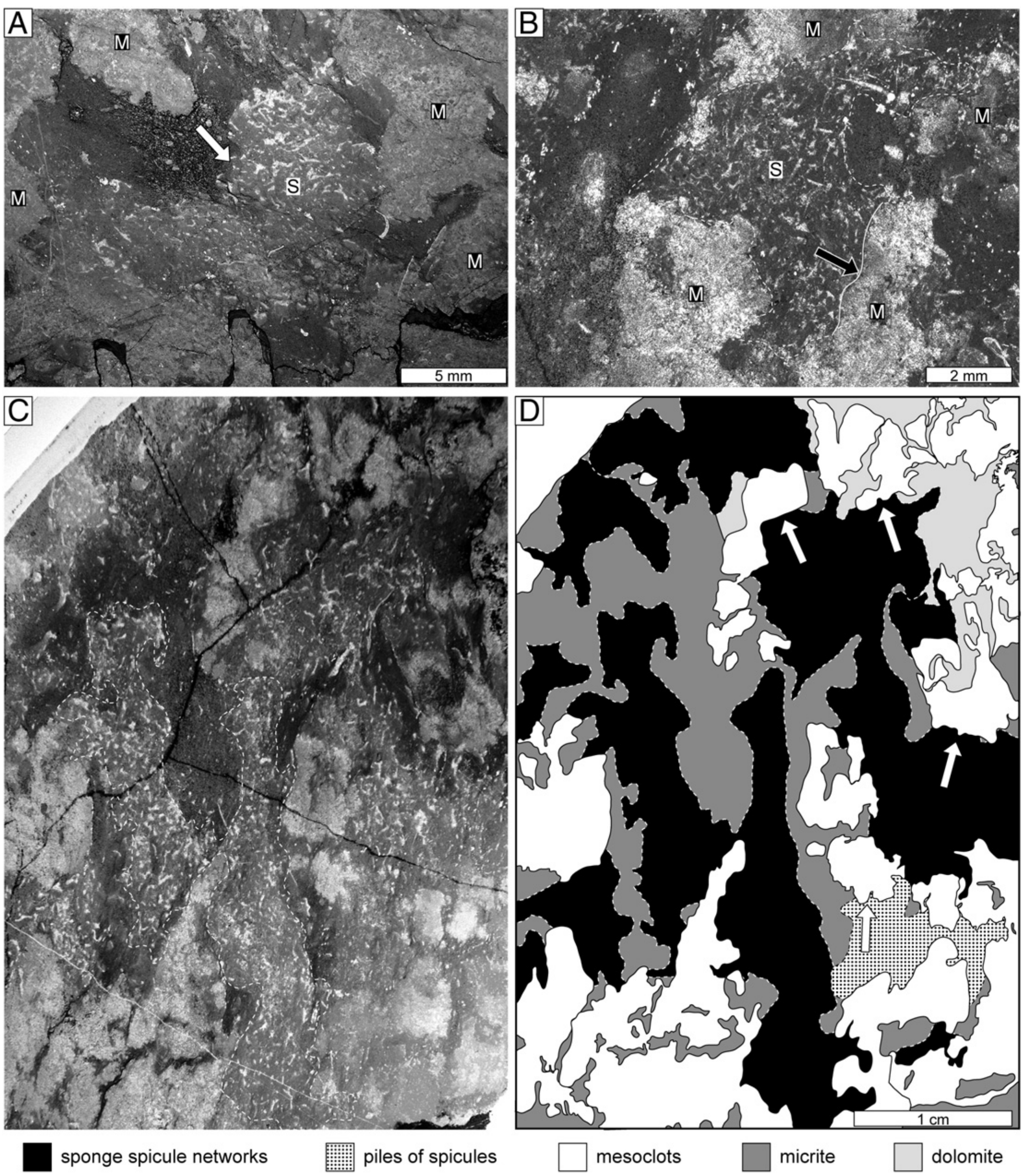

Fig. 5. Textures of the thrombolite-sponge boundstone. (A) Photomicrograph of irregular-shaped spicule network with indistinct outline (white arrow) surrounded by micrite and mesoclots. (B) Photomicrograph of irregular-shaped sponge remains overlying, laterally adjoining (black arrow) and overlain by mesoclots. (C, D) Photomicrograph and interpretive tracing of sponges intermingled with mesoclots and micrites. Some mesoclots appear attached to the top of sponges (white arrows). M = mesoclots; S = sponges. Refer to Fig. 2 for sample locations.

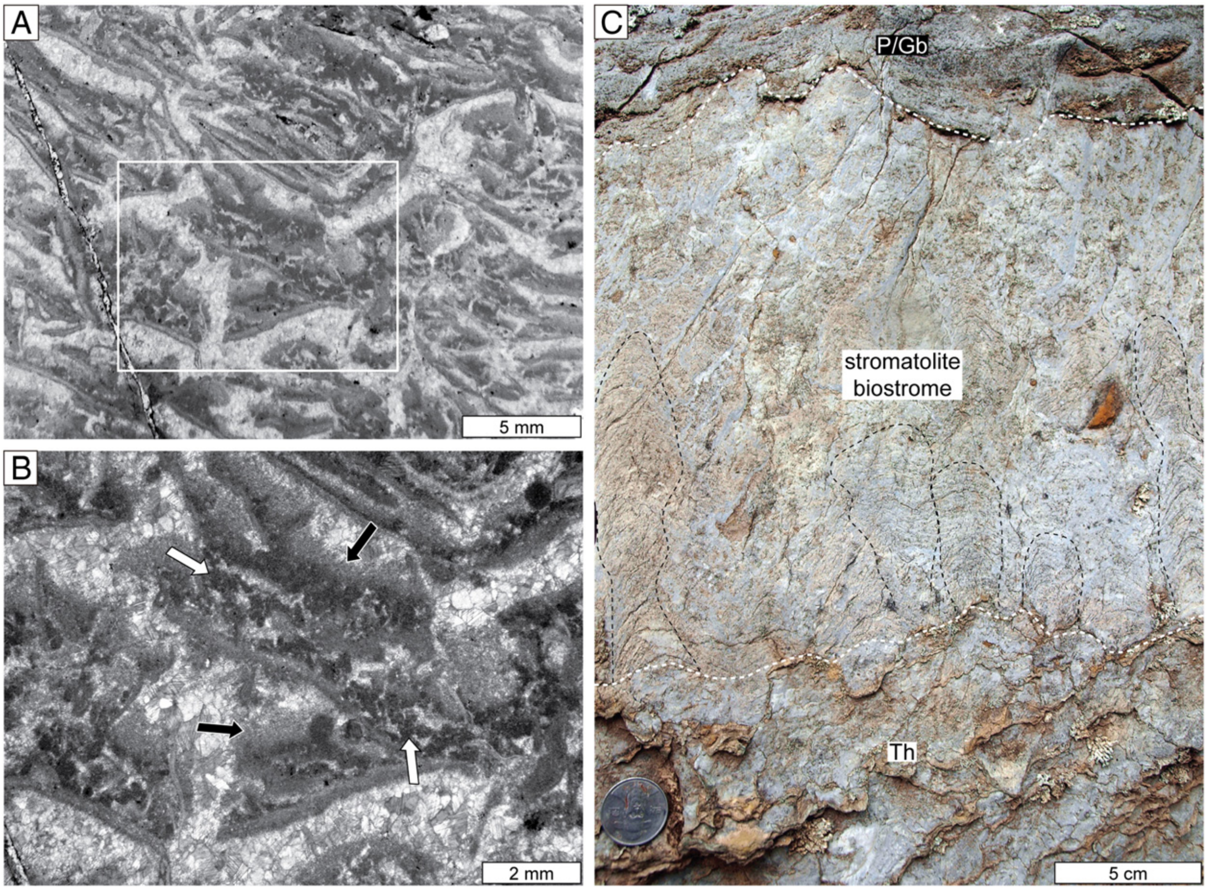

Fig. 6. (A) Photograph of *Girvanella* crust-*Epiphyton* boundstone showing dominance of stacked sheet-like to arcuate micritic masses and elongated spar cements. (B) Photomicrograph of rectangle in Fig. 6A showing darker *Epiphyton* thalli (white arrows) encrust on top of *Girvanella* crusts and are covered by light grey micritic internal sediments (black arrows). Th = thrombolitic reef, P/Gb = bioclastic packstone to grainstone. Refer to Fig. 2 for sample locations.

crusts (Fig. 6B). These *Epiphyton* are, in turn, blanketed by lime mud, with some growing upward to the base of the overlying *Girvanella* crusts. The rest of the boundstone is composed of minor trilobite and eocrinoid fragments and spar cement. A single 20 cm thick stromatolite biostrome occurs at 46 m above the base of the formation; it rests on a thrombolite-sponge reef at a truncation surface, and is overlain by bioclastic grainstone facies (Fig. 6C). Laterally linked to closely spaced (1–3 cm) columnar stromatolites 3–7 cm wide and 12–15 cm tall grade upward into upward-widening stromatolites with micritic walls, with lime mud filling the inter-columnar space. The stromatolite biostrome contains no recognizable calcimicrobes.

3.3. Interpretations

The Daegi Formation was deposited in a shallow subtidal environment dominated by carbonate sediments lacking intertidal to supratidal features (e.g., microbial laminites, dessication cracks, and precipitation mineral pseudomorphs) (Hong et al., in press). The middle part of the Daegi Formation ranges from platform margin environment dominated by bioclastic grainstone and ooid packstone to grainstone facies and low-energy platform interior environment behind platform margin grainstone belt with bioclastic wackestone to packstone (Table 1; Fig. 7). On the other hand, the lower and upper parts of the Daegi Formation encompass shale-dominated outer platform and grainstone-dominated platform margin environments, respectively (Fig. 7) (Hong et al., in press).

The Daegi reefs are an integral element of the Cambrian Series 3 carbonate platform deposits, primarily formed from behind of shoal grainstone belt to platform interior environments (Fig. 7). Intercalated bioclastic grainstone and ooid packstone to grainstone facies represent subtidal high-energy platform margin shoal deposits, while bioclastic wackestone to packstone facies represents deposition under lower-energy back-shoal to inner platform conditions (e.g., Kennard and James, 1986; Waters, 1989; Srinivasan and Walker, 1993; Osleger and Montañez, 1996; Read and Pfeil, 1983; de Wet et al., 2004; Woo et al., 2008; Hong et al., in press) (Table 1).

The Daegi thrombolite-sponge reefs comprise 91% ($n = 29/32$) of the reefs in this study. In addition, the observation that sponges constitute, on average, 9% of the thrombolite-sponge boundstone indicates their near ubiquitous existence within the studied thrombolitic reefs. Subordinate *Girvanella* crust–*Epiphyton* reefs also developed in environments comparable to those of thrombolite-sponge reefs, based on similar intercalated facies (e.g., James, 1981; Pratt, 1989; Srinivasan and Walker, 1993) (Table 2). The recurrence of numerous thrombolite-sponge reefs in the 100 m thick studied interval of the formation suggests that conditions optimal for their development persisted throughout the sequence, without significant perturbation (cf. Arp et al., 2001; Rowland and Shapiro, 2002). The absence of reefs in platform-margin to outer platform environments of lower and upper Daegi Formation suggests their environment-selective development (Fig. 7).

The Daegi thrombolite-sponge reefs are constructed primarily of the mesoclot-forming calcimicrobe *Epiphyton* and amalgamations of microbial clots. Lithistids occur in the interstitial space between mesoclots and *Epiphyton* clots and minor non-lithistid demosponges are surrounded by microbial clusters within the boundstone. These sponges are interpreted as dwellers of reefs that are principally microbial in composition (Kruse and Reitner, 2014; Adachi et al., 2015). Some lithistid sponges surrounded by mesoclots might have restricted

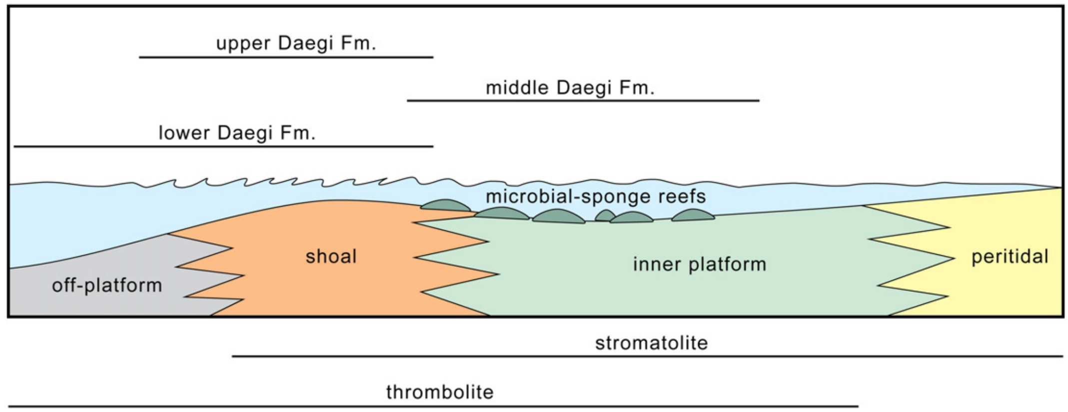

Fig. 7. Schematic depositional model of a Cambrian Series 3 carbonate platform. Approximate depositional windows of lower, middle and upper parts of the Daegi Formation are plotted. Microbial-sponge reefs of the Daegi Formation are mainly distributed in inner platform settings. Platform-wide distribution of stromatolite and thrombolite of the Cambrian Series 3 are shown below (summarized from Lee et al., 2015, table 1 and references therein).

lateral growth of the microbial mass and/or offered a substrate for microbial encrustation and growth, indicating incorporation of sponges to the microbial frameworks (Hong et al., 2012). The Daegi and coeval Zhangxia microbial reefs of eastern China (Adachi et al., 2015; Lee et al., in press), Sino-Korean Block, collectively represent one of the oldest microbial–lithistid sponge reefs of early Palaeozoic age, occurring within ca. 3.5 m.y. of the advent of lithistid sponge, and less than 5 m.y. after the decline of microbial–archaeocyath reef systems (Hong et al., 2012; Adachi et al., 2015; Lee et al., in press).

4. Discussion

4.1. Implications of microbial-sponge reefs on the Cambrian Series 3 carbonate depositional system

Archaeocyath-microbial reefs were the first microbial-metazoan reef-building association that flourished globally (James and Wood, 2010). Six different types of archaeocyath-microbial associations recognized by Gandin and Debrenne (2010) occurred in different

Table 2
Occurrence of latest Cambrian Series 2–Series 3 reefs. T: thrombolite; S: stromatolite; D: dendrolite; C: crust boundstone; *Gi*: *Girvanella*; *Ep*: *Epiphyton*; *Re*: *Renalcis*; *An*: *Angusticellularia*; *Ta*: *Taninia*; *Ko*: *Kordephyton*; Ss: scattered sponge spicules; Sl: lithistid sponge; Sd: non-lithistid demosponge; Sh: heteractinide sponge; Cn: stem-group cnidarian. Refer to Fig. 8 for reef locations.

Formation/location	Age	Occurrence	Dimension	Depositional environment	Reference	Reef location no.
Cow Head Group; Newfoundland, Canada	Guzhangian–Stage 10	C mound; *Gi*, *Ep*, and *Re*	N/A	Platform margin	James, 1981	21
Waterfowl Fm., Alberta, Canada	Guzhangian	T and D mound/ biostrome; *Re* and *Gi*	0.3–1.2 m high, 1 m wide, 1–10 m long	Shallow subtidal to intertidal	Waters, 1989	18
Zhangxia Fm., Shandong, China	Stage 5–Guzhangian	S reef/biostrome T and D mound; *Ep*, *Re*, *Gi*, Sl, Sd, and Cs	cm- to dm-scale ~several tens of m thick	Shallow subtidal	Woo et al., 2008; Woo, 2009; Adachi et al., 2015; Lee et al., in press	12
Daegi Fm., Korea	Drumian–Guzhangian	T mound; *Ep*, Sl, Sd and Cs	~12 m high	Shallow subtidal	Hong et al., 2012; Park et al. in press; this study	13
Maryville Ls., Tennessee, USA	Drumian–Guzhangian	T mound; *Re*, *Gi* and Ss	~15 m high	Platform margin	Srinivasan and Walker, 1993	20
Petit Jardin Fm., Newfoundland, Canada	Drumian–Guzhangian	T–S mound	~5 m high	Low-energy subtidal	Kennard and James, 1986	21
Ranken Ls., Northern Territory, Australia	Drumian	S reef; *An*, *Ta* & Sl	N/A	High-energy subtidal	Kruse and Reitner, 2014	15
Rockslide Fm., Northwest Territories, Canada	Drumian	C mound; *Gi* and *Ep*	25 m high, 120 m wide	Continental slope	Pratt, 1989	17
Wirrealpa and Aroona Creek ls., Flinders Ranges, Australia	Stage 5–Drumian	S mound	~8 m high	Lagoon	Youngs, 1978	15
Deh–Sulfiyan Fm., Iran	Stage 5–Drumian	S mound T mound	m-scale	Shallow subtidal to lower intertidal Shallow subtidal	Bayet-Goll et al., 2014	16
Bonanza King Fm., California, Nevada, Utah, USA	Stage 5–Drumian	T and S mound/ biostrome; *Ep*	dm- to m-scale	Platform margin	Rees, 1986; Osleger and Montañez, 1996	19
Mantou Fm., Shandong, China	Stage 5	T reef	Several cm high, several dm wide	Shallow subtidal	Lee and Chough, 2011	12
Qinjiamiao Fm., Hubei, China	lower Series 3	S reef	N/A	N/A	Adachi et al., 2014	14
Stephen Fm., Alberta, Canada	Stage 5	S	N/A	Platform margin	Aitken, 1967	18
Ledger Fm., Pennsylvania, USA	Stage 5	S and D biostrome; *Re*, *Go* & *Ta*	~0.5 m high	Platform margin	de Wet et al., 2004	20
Upper Shady Ds., Virginia, USA	Stage 5	T, D and C mound; *Ep*, *Re*, and *Gi*	1–60 m high	Platform margin	Read and Pfeil, 1983	20
Amga Fm., Sakha, Russia	Stage 5	T and D reef	N/A	N/A	Zhuravlev, 1996	22
Tindall Ls., Northern Territory, Australia	Stage 4–5	T reef; *Ko*, and Sh	2 m high, tens of m wide	N/A	Kruse and Reitner, 2014	15

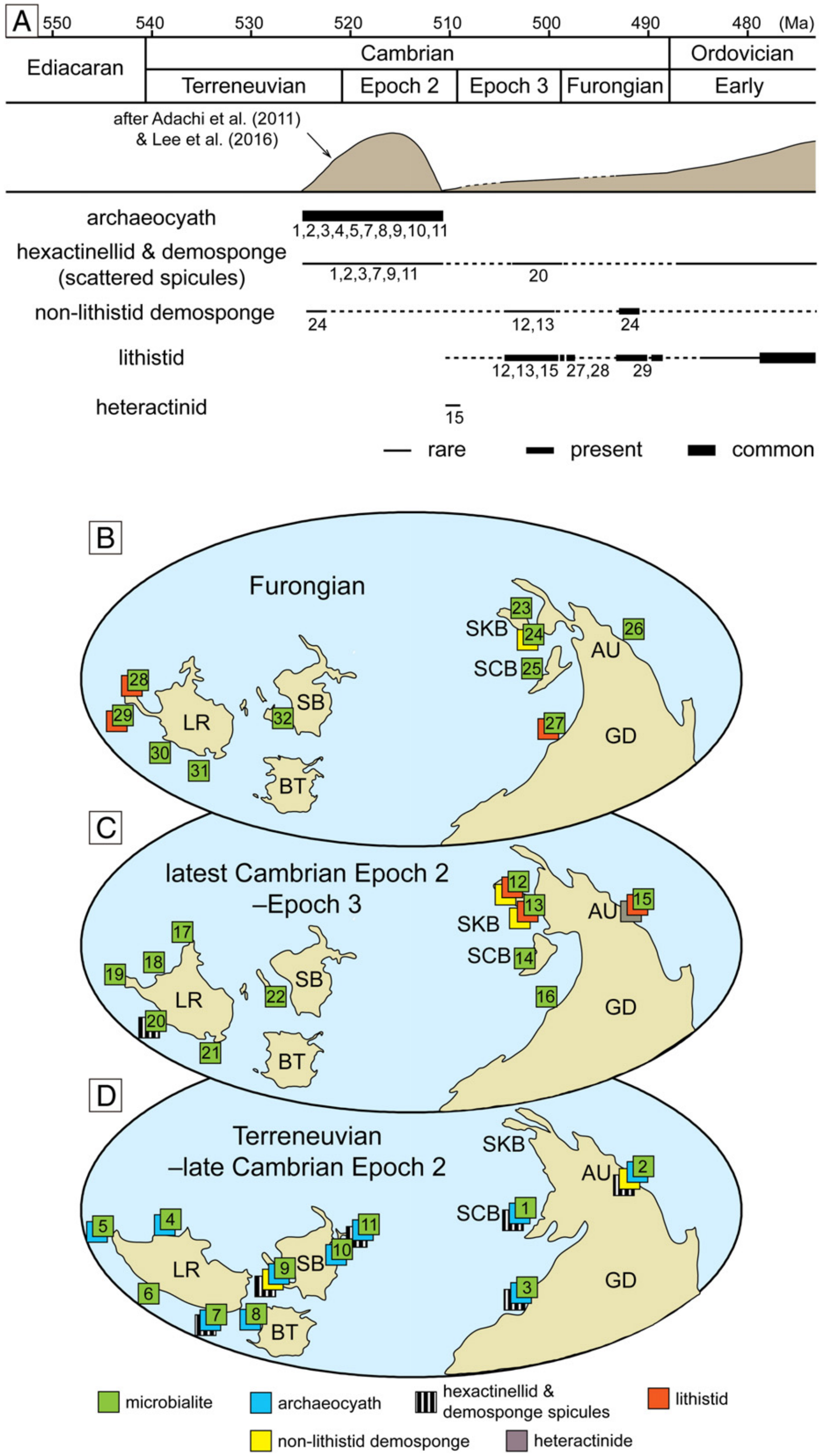

Fig. 8. Evolutionary trends (A) and palaeogeographic distributions (B–D) of Cambrian microbial reefs with metazoan components. Curves in (A) indicate temporal change in the relative abundance of microbial–metazoan reefs (Adachi et al., 2011; Lee et al., 2016). 1: Hicks and Rowland (2009); 2: James and Gravestock (1990); 3: Álvaro and Debrenne (2010); 4: Narbonne and Arbuckle (1989); 5: Rowland (1984); 6: Read and Pfeil (1983); 7: Kobluk and James (1979); James and Klappa (1983); 8: Elicki (1999); 9: Kruse et al. (1995); Luo (2015); 10: Zhuravlev (1996); 11: Wood et al. (1993); 12: Hong et al. (2012); Park et al. (in press) and this study; 13: Woo et al. (2008); Woo (2009); Lee and Chough (2011); Park et al. (2011); Adachi et al. (2015) and Lee et al. (in press); 14: Adachi et al. (2014); 15: Youngs (1978) and Kruse and Reitner (2014); 16: Bayet-Goll et al. (2014); 17: Pratt (1989); 18: Aitken (1967) and Waters (1989); 19: Rees (1986) and Osleger and Montañez (1996); 20: Read and Pfeil (1983); Srinivasan and Walker (1993) and de Wet et al. (2004); 21: James (1981) and Kennard and James (1986); 22: Zhuravlev (1996); 23: Lee et al. (2016); 24: Chen et al. (2011) and Lee et al. (2014); 25: Adachi et al. (2014); 26: Kennard and James (1986); 27: Kruse and Zhuravlev (2008); 28: Shapiro and Awramik (2000) and Shapiro and Rigby (2004); 29: Johns et al. (2007); 30: Demicco (1985) and Friedman (2000); 31: James (1981) and Hersi et al. (2002); 32: Zhuravlev (1996). Paleogeographic maps modified after Golonka (2007), Rowland and Shapiro (2002), and Blakey (2008). LR = Laurentia; SB = Siberia; GD = Gondwana; BT = Baltica; AU = Australia; SKB = Sino–Korean Block, SCB = South China.

environments, reflecting their adaption on diverse conditions including temperature, energy level, and depth, as well as morphology of the platform and its latitudinal position. They developed in various environmental settings throughout inner to outer shelf environments as well as platform margin, occupying both low- and high-energy conditions (Gandin and Debrenne, 2010). The archaeocyath-microbial associations are also often volumetrically important in the early Cambrian carbonate platform, sometimes forming ~100 m thick reef complex (James and Gravestock, 1990). Therefore, these earliest Phanerozoic reefs were important not only in terms of palaeoecology, but also in carbonate platform development.

On the other hand, the sponge-microbial reefs of Cambrian Series 3 and Furongian are usually small metre-scale mounds and much lesser in volume compared with microbial-dominated reefs, although their contribution on carbonate production is still not well understood (e.g., Shapiro and Rigby, 2004; Johns et al., 2007; Kruse and Zhuravlev, 2008; Kruse and Reitner, 2014; Adachi et al., 2015). Chen et al. (2014) showed that siliceous sponge-microbial reef-building association could have flourished throughout the Furongian of North China Platform in the form of maceriate reefs and suggested that they have played important roles in development of carbonate platform. However, due to their poor preservation and problems in taxonomy, further studies are required to understand these enigmatic reefs and their relationship with depositional environments (Lee et al., 2014, 2015).

The current study firstly demonstrates that in the aftermath of archaeocyath extinction, anthaspidellid sponges played important role in terms of carbonate sedimentation. Microbial-sponge reef-building association of the middle Daegi Formation occupied around half (~45%) of platform interior succession, with sponges constituting 9% of the boundstone. Such results imply their importance in carbonate production during the Cambrian Series 3. On the other hand, microbial-sponge reefs are generally absent from off platform margin to outer platform environments of the Daegi Formation, while microbial-dominant reefs of thrombolites and stromatolites flourished throughout much wider range of depositional environments during the Cambrian Series 3 (Fig. 7) (Lee et al., 2015, Table 1). Although further studies are required, this study implies that microbial-sponge reefs could have flourished in environments different from those of microbial reefs during the Cambrian Series 3.

4.2. Microbial-sponge reefs in the aftermath of archaeocyath extinction

Reef systems, which were dramatically disrupted by mass extinctions in the Phanerozoic, generally took up to several million years to recover from such events (Sheehan, 1985; Wood, 1999; James and Wood, 2010). In the case of the Late Devonian (Frasnian–Famenian) and Permian–Triassic extinctions, the microbial reefs reappeared immediately after the mass extinction events, and metazoans were often recruited into these microbial reefs (Wood, 1999; Flűgel and Kiessling, 2002). Recent discoveries demonstrate that some siliceous sponges immediately re-organized new reef consortia, and locally survived in reefs after the Late Devonian and end-Permian catastrophic extinctions (Wood, 2004; Brayard et al., 2011). After the decline of archaeocyaths in the late Cambrian Series 2, the ensuing Cambrian Series 3–Furongian reefs have generally been viewed as being of microbial-dominant types, with or without minimal contributions of metazoans (Zhuravlev, 1996; Pratt et al., 2001; Rowland and Shapiro, 2002).

Microbial–anthaspidellid sponge reefs were first noted from the lowest Furongian of Gondwana, in present-day Iran and were initially regarded as a local phenomenon (Hamdi et al., 1995; Rowland and Shapiro, 2002), until additional Cambrian Series 3 microbial reefs with metazoans were reported during the last decade, primarily from palaeoequatorial regions of Gondwana (Hong et al., 2012; Kruse and Reitner, 2014; Adachi et al., 2015) (Fig. 8A–C). Metre-scale Cambrian Series 3 reefs of the Sino–Korean Block of eastern China and Korea are built primarily by *Epiphyton*, mesoclots, and microstromatolites, with metazoans including conical anthaspidellid sponges, non-lithistid demosponges and stem-group cnidarians (Woo et al., 2008; Park et al., 2011; Hong et al., 2012; Adachi et al., 2015; Lee et al., in press). Australian stromatolitic reefs composed of microstromatolites, *Angusticellularia*, and *Taninia* contain planar to conical anthaspidellid sponges (Kruse and Reitner, 2014). In addition, stromatolite, maceriate and dendrolite reefs with anthaspidellid and non-lithistid demosponges, interpreted as dwellers and local framework builders, are described from the Furongian succession of Laurentia (western and southern USA) and Gondwana (eastern China) (Shapiro and Rigby, 2004; Johns et al., 2007; Kruse and Zhuravlev, 2008; Lee et al., 2014) (Fig. 8A–C) (Table 2).

Based on the preservation of partial siliceous sponges in reefs, and the difficulty of recognizing them in outcrop and on slabs, researchers of Cambrian Series 3–Furongian reefs have speculated that metazoans might have been much more common and widely distributed in these reefs than previously thought (Hong et al., 2012; Lee et al., 2014; Adachi et al., 2015). This study demonstrates the near ubiquitous distribution of lithistid sponges preserved as peloidal fabrics, spicule networks, and scattered spicules in Cambrian Series 3 thrombolitic reefs of the eastern Sino–Korean Block. Together with coeval Zhangxia microbial–sponge reefs of the central Sino–Korean Block (Adachi et al., 2015; Lee et al., in press), the data indicate a firmly entrenched relationship between thrombolite-building microbes and lithistid sponges, at least by the middle Cambrian Series 3 (Fig. 8A and C). It appears that the subsequent radiation of this type of reef toward Iran and North America in the Furongian (Fig. 8B–C) led to their cosmopolitan appearance during the Early Ordovician. Further studies on Cambrian Series 3–Furongian reefs will certainly help us to understand when and how metazoans incorporated into microbial-dominated reefs after extinction of archaeocyaths.

5. Conclusions

Cambrian Series 3 microbial reefs from Korea, dominated by mesoclots and *Epiphyton* as well as siliceous sponges, extensively flourished in the platform interior environment of the middle Daegi Formation, where they constitute 45% of studied interval in thickness. The sponges occur in most (90%) thrombolitic reefs investigated in this study, where they comprise, on average, 9% of the thrombolite-sponge boundstone, indicating that they are ubiquitous component of the boundstone. This study demonstrates that siliceous sponges incorporated into microbial reefs of post-late Cambrian Series 2 microbial–archaeocyath reefs, significantly contributed to the generation of carbonate sediments and carbonate platform development. Further studies on other Cambrian Series 3 to Furongian carbonate platforms will help us to understand the impact of archaeocyath extinction on carbonate sedimentary environments and reshaping of post-archaeocyath depositional systems.

Acknowledgements

This study was supported by a Korea University Grant to JH and JHL, grants from the National Research Foundation of Korea to SJC (2015R1A2A2A01007063) and DJL (2013R1A2A2A01067612). We appreciate the thorough and constructive comments of two anonymous reviewers and J. Park of Korea University on an earlier version of the manuscript. We also thank M. Lee, N.G. Kim, and J.W. Jeon of Andong National University for assistance with the preparation of thin sections.

Appendix A. Supplementary data

Supplementary data associated with this article can be found in the online version at http://dx.doi.org/10.1016/j.sedgeo.2016.04.012. These data include the Google map of the most important areas described in this article.

References

Adachi, N., Ezaki, Y., Liu, J., 2011. Early Ordovician shift in reef construction from microbial to metazoan reefs. PALAIOS 26, 106–114.
Adachi, N., Nakai, T., Ezaki, Y., Liu, J., 2014. Late early Cambrian archaeocyath reefs in Hubei Province, South China: modes of construction during their period of demise. Facies 60, 703–717.
Adachi, N., Kotani, A., Ezaki, Y., Liu, J., 2015. Cambrian Series 3 lithistid sponge-microbial reefs in Shandong Province, North China: reef development after the disappearance of archaeocyaths. Lethaia 48, 405–416.
Aitken, J.D., 1967. Classification and environmental significance of cryptalgal limestones and dolomites, with illustrations from the Cambrian and Ordovician of southwestern Alberta. Journal of Sedimentary Petrology 37, 1163–1178.
Álvaro, J.J., Debrenne, F., 2010. The great Atlasian reef complex: an early Cambrian subtropical fringing belt that bordered west Gondwana. Palaeogeography, Palaeoclimatology, Palaeoecology 294, 120–132.
Arp, G., Reimer, A., Reitner, J., 2001. Photosynthesis-induced biofilm calcification and calcium concentrations in Phaneorozoic oceans. Science 292, 1701–1704.
Bayet-Goll, A., Geyer, G., Wilmsen, M., Mahboubi, A., Moussavi-Harami, R., 2014. Facies architecture, depositional environments, and sequence stratigraphy of the Middle Cambrian Fasham and Deh-Sufiyan formations in the central Alborz, Iran. Facies 60, 815–841.
Blakey, R.C., 2008. Gondwana paleogeography from assembly to breakup–A 500 m.y. odyssey. In: Fielding, C.R., Frank, T.D., Isbell, J.L. (Eds.), Resolving the Late Paleozoic Ice Age in Time and Space. Geological Society of America Special Papers 441, pp. 1–28.
Brayard, A., Vennin, E., Olivier, N., Bylund, K.G., Jenks, J., Stephen, D.A., Bucher, H., Hofmann, R., Goudemand, N., Escarguel, G., 2011. Transient metazoan reefs in the aftermath of the end-Permian mass extinction. Nature Geoscience 4, 693–697.
Chen, J., Chough, S.K., Han, Z., Lee, J.-H., 2011. An extensive erosion surface of a strongly deformed limestone bed in the Gushan and Chaomidian formations (late Middle Cambrian to Furongian), Shandong Province, China: sequence-stratigraphic implications. Sedimentary Geology 233, 129–149.
Chen, J., Lee, J.-H., Woo, J., 2014. Formative mechanisms, depositional processes, and geological implications of Furongian (late Cambrian) reefs in the North China Platform. Palaeogeography, Palaeoclimatology, Palaeoecology 414, 246–259.
Choi, D.K., Chough, S.K., Kwon, Y.K., Lee, S.B., Woo, J., Kang, I., Lee, H.S., Lee, S.M., Sohn, Y.J., Lee, D.-J., 2004. Taebaek Group (Cambrian–Ordovician) in the Seokgaejae section, Taebaeksan Basin: a refined lower Paleozoic stratigraphy in Korea. Geosciences Journal 8, 125–151.
Chough, S.K., 2013. Geology and Sedimentology of the Korean Peninsula. Elsevier, Amsterdam.
de Wet, C.B., Frey, H.M., Gaswirth, S.B., Mora, C.I., Rahnis, M., Bruno, C.R., 2004. Origin of meter-scale submarine cavities and herringbone calcite cement in a Cambrian microbial reef, Ledger Formation (U.S.A.). Journal of Sedimentary Research 74, 914–923.
Delgado, F., 1977. Primary textures in dolostones and recrystallized limestone: a technique for their microscopic study. Journal of Sedimentary Petrology 47, 1339–1341.
Demicco, R.V., 1985. Platform and off-platform carbonates of the Upper Cambrian of western Maryland, U.S.A. Sedimentology 32, 1–22.
Elicki, O., 1999. Palaeoecological significance of calcimicrobial communities during ramp evolution: an example from the Lower Cambrian of Germany. Facies 41, 27–40.
Flűgel, E., 2010. Microfacies of Carbonate Rocks: Analysis, Interpretation and Application. Springer, Berlin.
Flűgel, E., Kiessling, W., 2002. Patterns of Phanerozoic reef crises. In: Kiessling, W., Flügel, E., Golonka, J. (Eds.), Phanerozoic Reef Patterns. SEPM, Tulsa, pp. 691–733.
Folk, R.L., 1987. Detection of organic matter in thin-sections of carbonate rocks using a white card. Sedimentary Geology 54, 193–200.
Friedman, G.M., 2000. Late Cambrian cabbage-head stromatolites from Saratoga Springs, New York, USA. Carbonates and Evaporites 15, 37–48.
Gandin, A., Debrenne, F., 2010. Distribution of the archaeocyath-calcimicrobial bioconstructions on the early Cambrian shelves. Palaeoworld 19, 222–241.
Geyer, G., Shergold, J.H., 2000. The quest for internationally recognized divisions of Cambrian time. Episodes 23, 188–195.
Golonka, J., 2007. Phanerozoic paleoenvironment and paleolithofacies maps: early Paleozoic. Geologica 35, 589–654.
Hamdi, B., Rozanov, A.Y., Zhuravlev, A.Y., 1995. Latest Middle Cambrian metazoan reef from northern Iran. Geological Magazine 132, 367–373.
Hersi, O.S., Lavoie, D., Nowlan, G.S., 2002. Stratigraphy and sedimentology of the Upper Cambrian Strites Pond Formation, Philipsburg Group, southern Quebec, and implications for the Cambrian platform in eastern Canada. Bulletin of Canadian Petroleum Geology 50, 542–565.
Hicks, M., Rowland, S.M., 2009. Early Cambrian microbial reefs, archaeocyathan inter-reef communities, and associated facies of the Yangtze Platform. Palaeogeography, Palaeoclimatology, Palaeoecology 281, 137–153.
Hong, J., Cho, S.-H., Choh, S.-J., Woo, J., Lee, D.-J., 2012. Middle Cambrian siliceous sponge-calcimicrobe buildups (Daegi Formation, Korea): metazoan buildup constituents in the aftermath of the Early Cambrian extinction event. Sedimentary Geology 253–254, 47–57.
Hong, J., Choh, S.-J., Lee, D.-J., 2016. Distribution of chancelloriids in a middle Cambrian carbonate platform deposit, Taebaek Group, Korea. Acta Geologica Sinica-English Edition(in press).
Howell, J., Woo, J., Chough, S.K., 2011. Dendroid morphology and growth patterns: 3-D computed tomographic reconstruction. Palaeogeography, Palaeoclimatology, Palaeoecology 299, 335–347.
James, N.P., 1981. Megablocks of calcified algae in the Cow Head Breccia, western Newfoundland: vestiges of a Cambro-Ordovician platform margin. Geological Society of America Bulletin 92, 799–811.
James, N.P., Gravestock, D.I., 1990. Lower Cambrian shelf and shelf margin buildups, Flinders Ranges, South Australia. Sedimentology 37, 455–480.
James, N.P., Klappa, C.F., 1983. Petrogenesis of Early Cambrian reef limestones, Labrador, Canada. Journal of Sedimentary Petrology 53, 1051–1096.
James, N.P., Wood, R., 2010. Reefs. In: James, N.P., Dalrymple, R.W. (Eds.), Facies Models 4. Geological Association of Canada, St. John's, pp. 421–447.
Johns, R.A., Dattilo, B.F., Spincer, B., 2007. Neotype and redescription of the Upper Cambrian anthaspidellid sponge, *Wilbernicyathus donigani* Wilson, 1950. Journal of Paleontology 81, 435–444.
Kang, I., Choi, D.K., 2007. Middle Cambrian trilobites and biostratigraphy of the Daegi Formation (Taebaek Group) in the Seokgaejae section, Taebaeksan Basin, Korea. Geosciences Journal 11, 279–296.
Kennard, J.M., James, N.P., 1986. Thrombolites and stromatolites: two distinct types of microbial structures. PALAIOS 1, 492–503.
Kobluk, D.R., James, N.P., 1979. Cavity-dwelling organisms in Lower Cambrian patch reefs from southern Labrador. Lethaia 12, 193–218.
Kruse, P.D., Reitner, J.R., 2014. Northern Australian microbial-metazoan reefs after the mid-Cambrian mass extinction. Australasian Paleontologists Memoirs 45, 31–53.
Kruse, P.D., Zhuravlev, A.Y., 2008. Middle–Late Cambrian *Rankenella–Girvanella* reefs of the Mila Formation, northern Iran. Canadian Journal of Earth Sciences 45, 619–639.
Kruse, P.D., Zhuravlev, A.Y., James, N.P., 1995. Primordial metazoan-calcimicrobial reefs: Tommotian (Early Cambrian) of the Siberian Platform. PALAIOS 10, 291–321.
Kwon, Y.K., Chough, S.K., Choi, D.K., Lee, D.-J., 2006. Sequence stratigraphy of the Taebaek Group (Cambrian–Ordovician), mideast Korea. Sedimentary Geology 192, 19–55.
Lee, H.S., Chough, S.K., 2011. Depositional processes of the Zhushadong and Mantou formations (early to middle Cambrian), Shandong Province, China: roles of archipelago and mixed carbonate-siliciclastic sedimentation on cycle genesis during initial flooding of the North China Platform. Sedimentology 58, 1530–1572.
Lee, J.-H., Chen, J., Choh, S.-J., Lee, D.-J., Han, Z., Chough, S.K., 2014. Furongian (late Cambrian) sponge-microbial maze-like reefs in the North China Platform. PALAIOS 29, 27–37.
Lee, J.-H., Chen, J., Chough, S.K., 2015. The Middle–Late Cambrian reef transition and related geological events: a review and new view. Earth-Science Reviews 145, 66–84.
Lee, J.-H., Hong, J., Woo, J., Oh, J.-R., Lee, D.-J., Choh, S.-J., 2016. Reefs in the early Paleozoic Taebaek Group, Korea: a review. Acta Geologica Sinica-English Edition 90, 352–367.
Lee, J.-H., Woo, J., Lee, D.-J., 2016. The earliest reef-building anthaspidellid sponge *Rankenella zhangxianensis* n. sp. from the Zhangxia Formation (Cambrian Series 3), Shandong Province, China. Journal of Paleontology(in press).
Luo, C., 2015. "Keratose" Sponge Fossils and Microbialites: a Geobiological Contribution to the Understanding of Metazoan Origin Ph.D. dissertation University of Göttingen, Göttingen, Germany.
Luo, C., Reitner, J., 2014. First report of fossil "keratose" demosponges in Phanerozoic carbonates: preservation and 3-D reconstruction. Naturwissenschaften 101, 467–477.
McKenzie, N.R., Hughes, N.C., Myrow, P.M., Choi, D.K., Park, T.-Y., 2011. Trilobites and zircons link North China with the eastern Himalaya during the Cambrian. Geology 39, 591–594.
Meng, X., Ge, M., Tucker, M.E., 1997. Sequence stratigraphy, sea-level changes and depositional systems in the Cambro-Ordovician of the North China carbonate platform. Sedimentary Geology 114, 189–222.
Narbonne, G.M., Arbuckle, S.M., 1989. Lower Cambrian algal–archaeocyathan reef mounds from the Wernecke Mountains, Yukon Territory. In: Geldsetzer, H.H.J., James, N.P., Tebbutt, G.E. (Eds.), Reefs, Canada and Adjacent Area. Canadian Society of Petroleum Geologists, Calgary, pp. 156–160.
Osleger, D.A., Montañez, I.P., 1996. Cross-platform architecture of a sequence boundary in mixed siliciclastic-carbonate lithofacies, Middle Cambrian, southern Great Basin, USA. Sedimentology 43, 197–217.
Park, T.-Y., Han, Z., Bai, Z., Choi, D.K., 2008. Two Middle Cambrian trilobite genera, *Cyclolorenzella* Kobayashi, 1960 and *Jiulongshania* gen. Nov., from Korea and China. Alcheringa 32, 247–269.
Park, T.-Y., Woo, J., Lee, D.-J., Lee, D.-C., Lee, S.-B., Han, Z., Chough, S.K., Choi, D.K., 2011. A stem-group cnidarian described from the mid-Cambrian of China and its significance for cnidarian evolution. Nature Communications 2, 442. http://dx.doi.org/10.1038/ncomms1457.
Park, T.-Y., Kihm, J.-H., Woo, J., Zhen, Y.-Y., Engelbretsen, M., Hong, J., Choh, S.-J., Lee, D.-J., 2016. Cambrian stem-group cnidarians with a new species from the Cambrian Series 3 of the Taebaeksan Basin, Korea. Acta Geologica Sinica-English Edition(in press).
Peng, S., Babcock, L.E., Cooper, R.A., 2012. The Cambrian Period. In: Gradstein, F.M., Ogg, J.G., Schmitz, M., Ogg, G. (Eds.), The Geologic Time Scale 2012. Elsevier, Amsterdam, pp. 437–488.
Pratt, B.R., 1989. Deep-water *Girvanella–Epiphyton* reef on a mid-Cambrian continental slope, Rockslide Formation, Mackenzie Mountains, Northwest Territories. In: Geldsetzer, H.H.J., James, N.P., Tebbutt, G.E. (Eds.), Reefs, Canada and Adjacent Area. Canadian Society of Petroleum Geologists, Calgary, pp. 161–164.
Pratt, B.R., Spincer, B.R., Wood, R.A., Zhuravlev, A.Y., 2001. Ecology and evolution of Cambrian reefs. In: Zhuravlev, A.Y., Riding, R. (Eds.), Ecology of the Cambrian Radiation. Columbia University Press, New York, pp. 254–274.
Read, J.F., Pfeil, R.W., 1983. Fabrics of allochthonous reefal blocks, Shady Dolomite (Lower to Middle Cambrian), Virginia Appalachians. Journal of Sedimentary Petrology 53, 761–778.
Rees, M.N., 1986. A fault-controlled trough through a carbonate platform: the Middle Cambrian House Range embayment. Geological Society of America Bulletin 97, 1054–1069.
Riding, R., 2000. Microbial carbonates: the geological record of calcified bacterial-algal mats and biofilms. Sedimentology 47, 179–214.
Riding, R., Zhuravlev, A.Y., 1995. Structure and diversity of oldest sponge-microbe reefs: Lower Cambrian, Aldan River, Siberia. Geology 23, 649–652.

Rowland, S.M., 1984. Were there framework reefs in the Cambrian? Geology 12, 181–183.
Rowland, S.M., Shapiro, R.S., 2002. Reef patterns and environmental influences in the Cambrian and earliest Ordovician. In: Kiessling, W., Flügel, E., Golonka, J. (Eds.), Phanerozoic Reef Patterns. SEPM, Tulsa, pp. 95–128.
Shapiro, R.S., Awramik, S.M., 2000. Microbialite morphostratigraphy as a tool for correlating Late Cambrian-Early Ordovician sequences. Journal of Geology 108, 171–180.
Shapiro, R.S., Rigby, J.K., 2004. First occurrence of an *in situ* anthaspidellid sponge in a dendrolite mound (Upper Cambrian; Great Basin, USA). Journal of Paleontology 78, 645–650.
Sheehan, P.M., 1985. Reefs are not so different–they follow the evolutionary pattern of level-bottom communities. Geology 13, 46–49.
Sim, M.S., Lee, Y.I., 2006. Sequence stratigraphy of the Middle Cambrian Daegi Formation (Korea), and its bearing on the regional stratigraphic correlation. Sedimentary Geology 191, 151–169.
Srinivasan, K., Walker, K.R., 1993. Sequence stratigraphy of an intrashelf basin carbonate ramp to rimmed platform transition: Maryville Limestone (Middle Cambrian), southern Appalachians. Geological Society of America Bulletin 105, 883–896.
Waters, B.B., 1989. Upper Cambrian *Renalcis–Girvanella* framestone mounds, Alberta. In: Geldsetzer, H.H.J., James, N.P., Tebbutt, G.E. (Eds.), Reefs, Canada and Adjacent Area. Canadian Society of Petroleum Geologists, Calgary, pp. 165–170.
Woo, J., 2009. Depositional Environments and Microbial Sedimentation of the Zhangxia Formation (Middle Cambrian) Ph.D. dissertation Seoul National University, Seoul, Korea.
Woo, J., Chough, S.K., Han, Z., 2008. Chambers of *Epiphyton* thalli in microbial buildups, Zhangxia Formation (Middle Cambrian), Shandong Province, China. PALAIOS 23, 55–64.
Wood, R., 1999. Reef Evolution. Oxford University Press, Oxford.
Wood, R., 2004. Palaeoecology of a post-extinction reef: Famennian (Late Devonian) of the Canning Basin, north-western Australia. Palaeontology 47, 415–445.
Wood, R., Zhuravlev, A.Y., Anaaz, C.T., 1993. The ecology of Lower Cambrian buildups from Zuune Arts, Mongolia: implications for early metazoan reef evolution. Sedimentology 40, 829–858.
Youngs, B.C., 1978. The petrology and depositional environments of the Middle Cambrian Wirrealpa and Aroona Creek limestones (South Australia). Journal of Sedimentary Petrology 48, 63–74.
Zhuravlev, A.Y., 1996. Reef ecosystem recovery after the Early Cambrian extinction. In: Hart, M.B. (Ed.), Biotic Recovery from Mass Extinction Events. Geological Society, London, pp. 79–96.